SCIENCE CHINA
Earth Sciences

• RESEARCH PAPER •

December 2012 Vol.55 No.12: 2058–2067
doi: 10.1007/s11430-012-4374-7

# Preliminary multiproxy surface air temperature field reconstruction for China over the past millennium

SHI Feng[1,2], YANG Bao[1*] & Lucien Von GUNTEN[3]

[1] *Key Laboratory of Desert and Desertification, Cold and Arid Regions Environmental and Engineering Research Institute, Chinese Academy of Sciences, Lanzhou 730000, China;*
[2] *State Key Laboratory of Numerical Modeling for Atmospheric Sciences and Geophysical Fluid Dynamics (LASG), Institute of Atmospheric Physics, Chinese Academy of Sciences, Beijing 100029, China;*
[3] *Oeschger Centre for Climate Change Research & Institute of Geography, University of Bern, Bern, Switzerland*

Received July 25, 2012; accepted October 20, 2012

We present the first millennial-length gridded field reconstruction of annual temperature for China, and analyze the reconstruction for spatiotemporal changes and associated uncertainties, based on a network of 415 well-distributed and accurately dated climatic proxy series. The new reconstruction method is a modified form of the point-by-point regression (PPR) approach. The main difference is the incorporation of the "composite plus scale" (CPS) and "Regularized errors-in-variables" (EIV) algorithms to allow for the assimilation of various types of the proxy data. Furthermore, the search radius is restricted to a grid size; this restriction helps effectively exclude proxy data possibly correlated with temperature but belonging to a different climate region. The results indicate that: 1) the past temperature record in China is spatially heterogenic, with variable correlations between cells in time; 2) the late 20th century warming in China probably exceeds mean temperature levels at any period of the past 1000 years, but the temperature anomalies of some grids in eastern China during the Medieval climate anomaly period are warmer than during the modern warming; 3) the climatic variability in the eastern and western regions of China was not synchronous during much of the last millennium, probably due to the influence of the Tibetan Plateau. Our temperature reconstruction may serve as a reference to test simulation results over the past millennium, and help to finely analyze the spatial characteristics and the driving mechanism of the past temperature variability. However, the lower reconstruction skill scores for some grid points underline that the present set of available proxy data series is not yet sufficient to accurately reconstruct the heterogeneous climate of China in all regions, and that there is the need for more highly resolved temperature proxies, particularly in the Tibetan Plateau.

**climate change, global warming, paleoclimatology, temperature field reconstruction**

**Citation:** Shi F, Yang B, Gunten L V. Preliminary multiproxy surface air temperature field reconstruction for China over the past millennium. Sci China Earth Sci, 2012, 55: 2058–2067, doi: 10.1007/s11430-012-4374-7

Recent progress in the application of climate proxy data has demonstrated the possibility of reconstructing temporal climatic patterns for the past few centuries at the regional, continental [1–5] and global scale [6, 7]. Regional reconstructions have been made for Europe [8–12], North America [13], and South America [14, 15]. The information on spatial patterns of temperature variation over China available from the global reconstruction [6] is of limited use, because few proxy data are used in China: reconstructed grid points for China rely largely on interpolation from proxy data outside China. Moreover, currently there are only three temperature reconstructions using multi-proxy data for China and all these studies used a relatively small set of proxy records. Wang et al. [16] calculated a temperature

*Corresponding author (email: yangbao@lzb.ac.cn)

series over the past millennium for China by averaging ten regional multi-proxy series, Yang et al. [17] assembled nine proxy records to reconstruct temperature variation of the past 2000 years in China, and Ge et al. [18] also just used 23 proxy records.

Integrative regional temperature reconstruction series at sub-continental scale are available from many reliable climate archives in China [16–22]. A notable example is a tree-ring reconstruction of temperature and precipitation for the Tibetan Plateau over the past millennium [20, 23–26]. However, even though many well resolved proxy climate series exist, no gridded temperature field reconstruction has been produced for China so far.

The reconstruction of spatial large-scale temperature pattern for China is hindered by two obstacles. First, the complex spatial and temporal correlation structure of the climate system in China is hard to capture with traditional multi-proxy reconstruction methods (e.g., principal component analysis, PCA). The fundamental assumption of most field reconstruction methods is that the spatial modes of temperature variation for the long-term proxy record (e.g., the past 1000 years) follow those of the much shorter period covered by instrumental temperature. This implicit assumption of stationarity may not be satisfied because climate spatial mode can be affected by changes in the atmospheric circulation, solar activity, human activities, and other events, such as volcanic eruptions [27]. The second obstacle is that available climatic proxies in China are rare, unevenly distributed in space, and differ in length and sensitivity to temperature.

To address the first obstacle, we adopt a reconstruction approach that applies two reconstruction techniques, namely composite plus scale (CPS) and Regularized errors-in-variables (EIV), using a small search radius, such that each point is independently reconstructed. Such a locally-based approach to regional reconstruction is the essence of point-by-point regression (PPR) to allow for a "local control" of the reconstruction at each point [28]. A notable recent application of PPR is the development of the Monsoon Asia Drought Atlas (MADA) [29]. In this paper, we restrict the "search radius" for CPS and EIV to only one grid square to exclude proxy data that may be statistically correlated with temperature signal but belong to a different local climate region. This restriction is important because China has various climate regions associated with different features of atmospheric circulations (Westerlies, East Asian monsoon, and South Asian monsoon) and a complex climatology associated with the topographic influence of the Tibetan Plateau [30]. The application of both CPS and EIV allow the use of different proxy types, and thus to extend the application of the point-by-point regression approach. To address the second obstacle mentioned above, the scarcity and heterogeneity of proxy records, we use the largest set of proxy records from China used in a study so far. We assemble and screen the dataset, and only use records with a temporal resolution of finer than 30 years.

In this paper, we introduce a modified version of the PPR reconstruction method and apply it to a network of proxy data in China to generate a gridded reconstruction of annual temperature for the last 1000 years. We assess the reconstruction skills and describe the spatial temperature variations in China decadal to century timescales.

## 1 Data and methods

### 1.1 Instrumental data

We used the CRUTEM3v 5°×5° gridded instrumental surface-air temperature data set for the period 1850–2006 (Climatic Research Unit, Norwich, UK; www.cru.uea.ac.uk/cru/data/temperature) in China [31]. The CRUTEM3v dataset is highly correlated with the China Homogenized Historic Temperature dataset (CHHT; http://cdc.cma.gov.cn/home.do) [32] from 730 stations and with the average temperature series from ten regions in China [16] over the past 50 years (see Figure S1 in Appendix. http://earth.scichina.com; http://springerlink.com). Therefore, we use the CRUTEM3v dataset in this study as it is continuous (no gaps) and has the best spatial coverage of all available reanalysis datasets. However, the period 1850–1920 was not used in this study because before AD 1921 there are no instrumental data available for most of China (e.g., the Tibetan Plateau, Northwest, and Southwest) and the quality of the dataset cannot be assessed.

### 1.2 Climatic proxy data

We assembled 415 published proxy data series from China (see Figure 1(a)), following two essential criteria: the proxy data are used to reconstruct temperature in the peer-reviewed literature and have a time resolution of finer than 30 years. With the exception of tree rings, all proxy series used in this study have been previously used to reconstruct temperature or were validated as temperature records. For the tree ring records, the situation is more complex, as in some regions, tree rings have been shown to be sensitive to several climatic influences at different frequencies. Tree-ring chronologies from northern and western China are sensitive to drought [29], precipitation [33] or temperature [20, 34]. For example, the northwest China is classified as "arid and semiarid lands", which are reported to follow a "warm-wet" and "cold-dry" pattern in long-term climate trend [20, 35]. Accordingly, the low frequency variations of some tree-ring chronologies may reflect temperature variability at the large spatial scale [35]. At the large spatial resolution of our grid (5°×5°), it is very probably to interpret the low frequency variations in these chronologies as a temperature signal. In this reconstruction process, any proxy series was accepted only if it exhibited a roughly significant ($p$<0.13) correlation with instrumental surface temperature for either of the

two nearest grid points over the AD 1951–1996 calibration period. All tree-ring chronologies also had to cover at least the interval 1800 to 1970 and being built up from at least five samples in every year. Although the tree-ring series might represent different seasonal signals, some responding to summer temperature and some to annual temperature, they were all used to reconstruct mean annual temperature.

Data having a temporal resolution between 1 and 30 years were linearly interpolated to annual time steps [6, 29]. Such interpolation introduces significant bias by adding red-noise at the expense of high-frequency components of the spectrum, and thus to lower verification skill due to higher autocorrelation. Therefore, we limit our interpretation of the temperature reconstruction to decadal and longer timescales.

The problem with the tree-ring series is that the low-frequency (i.e., beyond the age of the tree) climate signal is not well conserved or, if present, needs to be statistically extracted from the raw data [36]. The regional curve standardization (RCS) is the better method to preserve the low-frequency signal from the raw data [36] than the traditional standard (STD) method and is used whenever possible in this study. However, most tree-ring series in the International Tree-Ring Data Bank (ITRDB) did not contain the "pith offset" information that is required to calculate RCS. In these cases, the STD chronologies were used in this study. Table S1 lists the proxy data and their characteristics (Table S1 in Appendix. http://earth.scichina.com; http://springerlink.com). The dataset includes 373 tree-ring chronologies, 15 historical documentary series, 6 speleothems series, 10 ice core series, and 11 temperature composite chronologies (local temperature reconstructions and multi-proxy data regional composite chronologies). All references of 415 proxies come from 43 papers [3, 17, 18, 20, 21, 25, 26, 37–71]. Our dataset includes the proxy records in China used for the hemispheric and global temperature reconstruction by Mann et al. [49], but we used the updated version of the Dasuopu, Dunde, and Guliya ice core records [55]. The following records were not used in this study as their temperature signal is questionable: the Dongge stalagmite record [72], the centennial-scale dry-wet variations from instrumental and documentary data of Qian et al. [73], and the isotimic lines record of first and last frosts, A.D. 1400–1900 in the Yellow River region [74]. Finally, we corrected the geographical positions of the historical documentary data [69]. Figure 1(b) shows the frequency of starting years back in time binned by century.

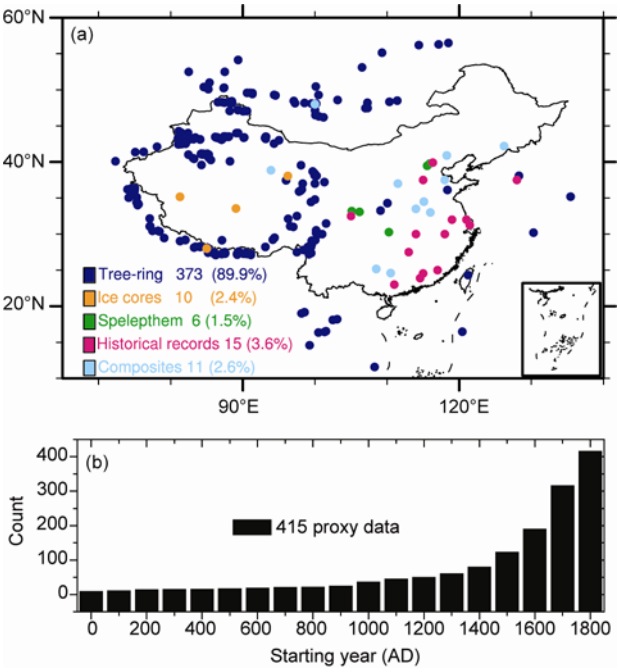


**Figure 1** (a) Map showing the study area and geographical locations of temperature proxy records used in this study. The dashed grid shows the 5° cells used for the reconstruction. (b) The frequency of starting years back in time binned by century.

### 1.3 Reconstruction method

The method of temperature reconstruction used in this study is a modified form of "point-by-point regression, PPR". PPR is a straightforward principal components regression method that has been successfully applied to produce high-quality reconstructions of droughts over North America [75], and to generate drought atlases for North America [13] and Asia [29].

PPR is based on the hypothesis that only proxy record close to the grid point to reconstruct can be good predictor at that location–a premise that is important in a region with a spatially heterogenic climate such as China. The original PPR approach optimizes the two variables "search radius" and "screening probability". The search radius defines the maximum distance used to find potential proxy data series and the screening probability defines the correlation threshold for retaining proxy series to be used to reconstruct temperature in that grid point [28].

All methods for reconstructing climate variability with proxy data can be expressed by:

$$T_k = BP + e_k, \tag{1}$$

where $T_k$ is the climatic data (e.g., temperature) at grid point $k$. $P$ is the proxy records, $B$ is the regression coefficients, and $e_k$ is the regression model errors [28]. In the PPR method, which was specifically developed for the analysis of tree-ring series, $P$ is the orthogonal tree-ring series principal component scores as

$$P = P_{TR}F, \tag{2}$$

where $P_{TR}$ is the matrix of standardized tree-ring chronologies used as predictors and $F$ is the orthonormal matrix of column eigenvectors calculated from the correlation matrix of $P_{TR}$ [28]. Our approach differs from the original PPR in the specifications of search radius, screening probability, and in the incorporation of two different regression tech-

niques: composite plus scaling (CPS) and regularized errors-in variables (EIV) to allow for the assimilation of non-tree ring data. The steps are described in more detail below.

Step 1: Processing of proxy data. We interpolated records with coarse resolution to annual resolution by cubic spline interpolation. Then, as the end years of some proxy data did not arrive at AD 1996, we extrapolated them to AD 1996 with the regularized expectation-maximization (RegEM) algorithm, based on the mutual covariance with the other available proxy data over the 1800–1996 interval [76]. Finally, to avoid bias due to some multi-proxy data with coarse resolution, all records were filtered to retain frequencies $f$<0.1 cycle per year to prepare the reconstruction.

Step 2: Screening of proxy data. A proxy series was accepted only if it exhibited a significant ($p$<0.13) correlation with instrumental surface temperature for either of the two nearest grid points over the AD 1951–1996 calibration period. The dense proxy network allowed a search radius of only one grid square. For example, the distance between the neighboring grid point 32.5°N/102.5°E and 32.5°N/110°E, and therefore the search radius is 703 km. This small search radius ensures that proxy data contributing to a grid point belong to the climate regime of the grid point, and that all grid cells are reconstructed using either the proxy data within the cell or from an adjacent cell.

Step 3: Splitting of proxy and instrumental data. Following the procedure described by Mann et al. [49], the screened proxy and instrumental data were separated into high-frequency/low-frequency bands with a Butterworth IIR filter with a 1/10 cycle per year cutoff frequency. The screened proxy data were separated into high and low frequency bands, and only low frequency band was preserved to reconstruct past temperature. This frequency split facilitates the assimilation of proxy data with differing temporal resolution.

Step 4: Regressing of proxy data. We use the multi-proxy reconstruction methods composite plus scaling (CPS) [49], and regularized errors-in-variables (EIV) [49], within the PPR framework to reconstruct past temperatures in the low frequency band. These techniques are described in detail elsewhere [6, 12, 49, 76–80]. With the small search radius, the approach used here shares reconstruction principles with the PPR method [28]. The main difference in this study is the use of CPS and EIV instead of principal components regression. Principal components regression underestimates the climate variability [78, 81].

For the CPS method, we use the variance matching approach [82, 83] to determine the transfer function, as:

$$T_k = \frac{(P - M_{P_{cal}}) \cdot S_{T_{cal}}}{S_{P_{cal}}} + M_{T_{cal}}, \quad (3)$$

where $T_{cal}$ represents the instrumental temperature during the calibration period, $P_{cal}$ represents the proxy data during the calibration period, $M$ is the average of the data, and $S$ is the standard deviation of the data. We combined multi-proxy data sets into one proxy data set $P$ with the same temporal resolution by low-pass filtering the data series to retain frequencies $f$<0.1 cycle per year. The advantage of this method is that it reduces the influence of large standard deviation in the proxy series.

In the EIV method, the RegEM algorithm [78, 80] was used to determine the regression coefficients B and regression model errors $e_k$, as:

$$T_k = P + (T_{cal} - P_{cal})B + e_k, \quad (4)$$

As a further safeguard against potentially non-robust results, a minimum of three predictors was required in implementing the Errors-in-Variables procedure[49].

Step 5: Validation of reconstruction. The accuracy and skill of grid-point reconstructions were summarized using a split-period approach [29, 49]. Reconstruction models were calibrated in the period 1951–1996 and validated on the period 1921–1950. Reconstruction skills were measured by the square of Pearson product-moment correlation coefficient ($r^2$), the reduction of error (RE) and the coefficient of efficiency (CE) statistics [29].

To account for the uncertainty introduced by the linear interpolation of the lower resolution proxy series, we only reconstructed temperatures in the low-frequency band. The reconstructed decadal average temperature anomalies for China over the past millennium were calculated as an average of all gridded reconstructions considering the land area weighting. Indeed, some grid points at the periphery of the study and over the sea area cover only a small proportion of land compared to grid points at the center of the research area. Furthermore, the reconstructed temperatures in each grid point were weighted with the cosine of their latitude. The average temperature anomalies for the eastern and western regions were calculated for all grid points East and West of 105°E considering the same area weighting.

## 2 Results and discussion

Reconstruction accuracy as measured by the squared correlation ($r^2$) varies greatly over the 58 grids, with a maximum of 0.84 and a median of 0.26 for the CPS results. Listed in Table S2 are the reduction of error (RE) with a maximum of 0.88 and median of 0.26 and coefficient of efficiency (CE) with a maximum of 0.58 and mean of –1.59 for CPS results (Table S2 in Appendix, http://earth.scichina.com, http:// springerlink.com). The results for EIV are similar with squared correlation ($r^2$) of 0.95 (median: 0.33), a maximum RE of 0.89 (median: –0.32) and a maximum CE of 0.68 (mean: –3.00). Overall, the RE values are high and 36(21) of 58 CPS (EIV) results pass the RE validation. These results show that our reconstruction has good skills. However, the CE values are generally relatively low, espe-

cially over the Tibetan Plateau and Tarim Basin. The reasons for these low values are unclear, but may be related to a limited amount of long instrumental and proxy records in these regions. We also test a sub-dataset excluding the tree ring data which were used to reconstruct MADA [29]. The spatial pattern coincided with the current results.

Figure 2(a) shows the reconstructed temperature anomalies (with respect to AD 1961–1990) over the last 1000 years in China using the CPS and EIV methods. The results are consistent with the reconstructions derived only from 36(21) of 58 CPS (EIV) gridpoint data which passed the RE validation. The grid points shown in Figure 2(a) cover the AD 1000–1996 period. The underlying shape of the reconstructed temperature averaged over China is an asymmetrical long wave that decreases gradually from a peak near AD 1040 to a low near AD 1500 and then increases more steeply to a maximum towards AD 1996 (Figure 2(a)). Almost the entire record is cooler than the AD 1961–1990 period used to calculate temperature anomalies. Cool excursions from the underlying wave are reconstructed in AD 1400–1460 and AD 1620–1640. A Little Ice Age (LIA) type event can be recognized in AD 1400–1700. The first warm period of the record (AD 1030–1280) is likely to be a regional expression of the Medieval Climate Anomaly (MCA). The second warmer period is AD 1540–1580 during the LIA. The third warm period in the mid-18th century with strong warming from AD 1700 to 1720 have been described previously [16]. The last decades of the record (AD 1924–1996) are warmer than any period of the past 1000 years.

Figure 2(b) shows the averaged EIV reconstructions over the eastern (105°–135°E) and western (70°–105°E) regions of China. The aforementioned long wave is also evident in the temperature series averaged over eastern and western gridpoints, although the amplitude is visibly larger in the West than in the East. However, the amplitude of the low-pass filtered instrumental temperature anomalies in the East after 1950 is higher (Figure S2 in Appendix. http://earth.scichina.com; http://springerlink.com). The East is much warmer than the West during the interval AD 1000–1100.

Figure 3 shows that our reconstruction is very similar to the results from other studies covering the past millennium [16, 17, 49], and that the transition periods from warm to cold conditions are identified during the same periods. Figure 4 shows the spatial temperature average anomalies patterns for the 11th to the 20th century with respect to AD 1961–1990. Maps of reconstructed temperature averaged over the centuries indicate that during the warm period of the 11th century, the temperature anomalies for entire China are positive, with the highest values in central and eastern China. The warming during the 12th to 13th centuries was also likely most pronounced in the central and eastern regions, whereas other regions of China, especially Xinjiang and the region northwest of the Tibetan Plateau, remained relatively colder (Figure 4). The 15th and relatively colder 16th centuries show a transition to somewhat cooler conditions, especially in the Northeast. Most regions of China were relatively cold during the 17th century. During the 18th century, temperatures in China raised again, most notably in the central and eastern regions. In the 19th century, temperature continue to raise over China. Finally, in the 20th century, temperatures raise throughout China, with more pronounced changes in the eastern and southern regions than in the northern and western regions.

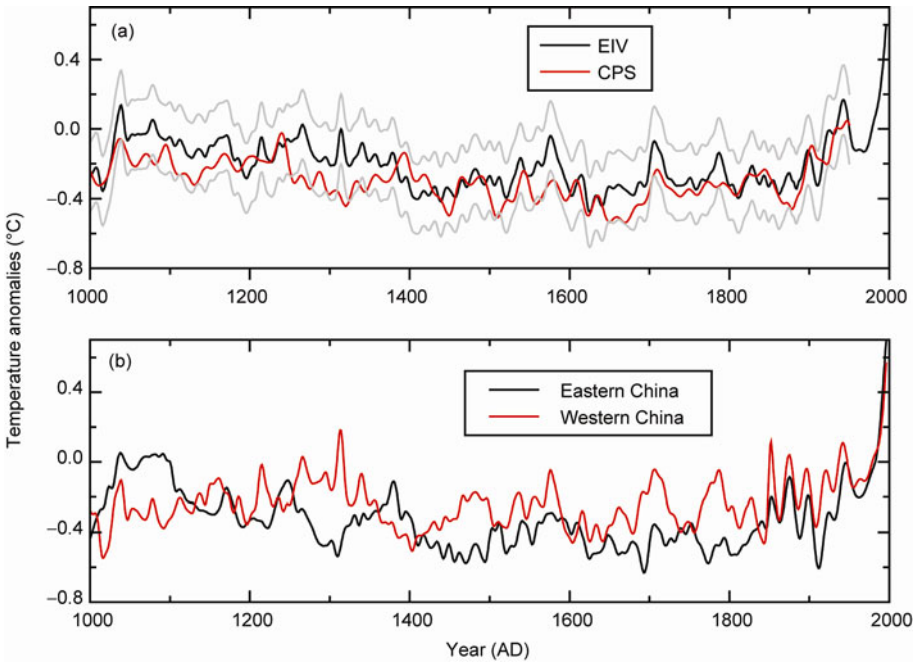


**Figure 2** Reconstructed temperature anomalies (with respect to AD 1961–1990) over the last 1000 years in China. (a) CPS (red line) and EIV (black line). Gray lines mark the uncertainty of the EIV reconstruction. (b) EIV Reconstructions averaged over eastern and western regions of China.

To illustrate the spatial structure of temperature variability at a finer time resolution, we present maps for six selected anomaly periods (Figure 5(a)–(f)): the first cold sixty consecutive years (AD 1400–1460) and the cold period AD 1620–1640, three warm periods (AD 1030–1080, 1230–1280 and 1700–1720), the documented extreme drought event of AD 1922–1932. The Little Ice Age type event of AD 1400–1460 and AD 1620–1640 were characterized by cold conditions in eastern China and relatively warmer conditions in southwest of the Tibetan Plateau (Figure 5(a) and (b)). This East-West contrast in temperature anomaly is also evident in the time series plots of Figure 5(c) and (d). As shown in Figure 4, the spatial structure of the warm period in the 13th century was similar with 11th century. The early-18th century warming is most prominent in the West, whereas the early 11th century warming is most apparent in the East.

The AD 1920s drought event [46] is clearly visible in Figure 5(f). This event affected the whole country, but especially the central and southwest regions. In some parts of the central China, the temperature anomalies were even higher than during the period AD 1980–1999 (see Figure 4(f)).

The instrumental data also illustrate the strong spatial and temporal variability between the gridded regions. As further evidence for the spatial variability, correlation coefficients between the grid point in the northeast Tibetan Plateau (102.5°E, 32.5°N), and the three grid points in the central Tibetan Plateau (92.5°E, 32.5°N; 87.5°E, 32.5°N; 82.5°E, 32.5°N) are all lower than 0.28. These low correlations probably reflect the varied topography of the Tibetan Plateau and its effect on climate.

Figure 6 shows the empirical orthogonal function (EOF) analysis of the averaged temperature anomalies of the EIV reconstruction for the years AD 1000–1996 and for the instrumental data in the period AD 1951–1996. The first EOF mode (EOF1) of the reconstruction explained 25.9% and the EOF1 of the instrumental data 63.8% of the total variance. The most likely reason for this large difference is that the proxy data cannot cover the entire spectrum of the temperature variability [27]. The first three EOF modes of reconstruction and observation are different. Most significantly, the first three EOF modes of the reconstruction data show

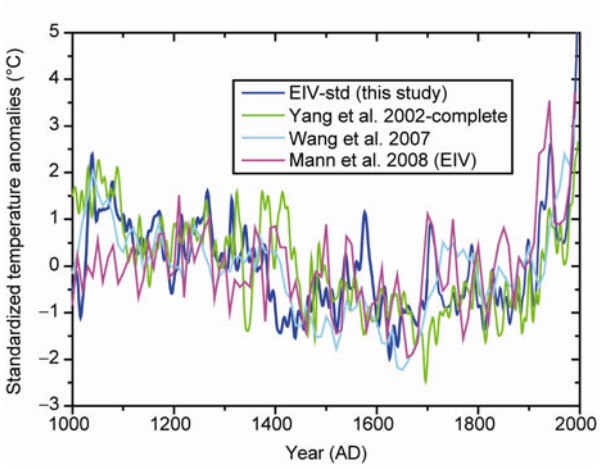


**Figure 3** Comparison of the EIV reconstruction for China of this study with three independent temperature reconstructions series for the past millennium. All temperature values are standardized to a mean of zero and a variance of one.

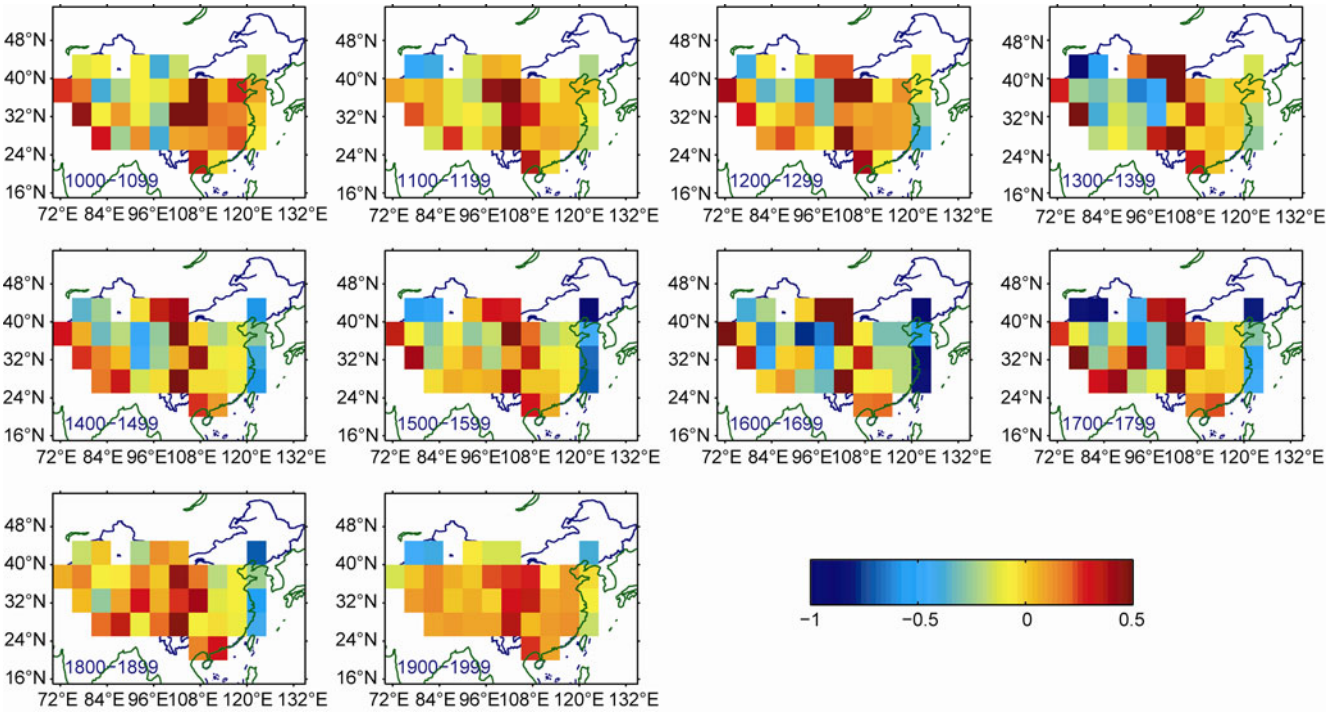


**Figure 4** Spatial temperature anomalies patterns from the 11th to the 20th century with respect to AD 1961–1990.

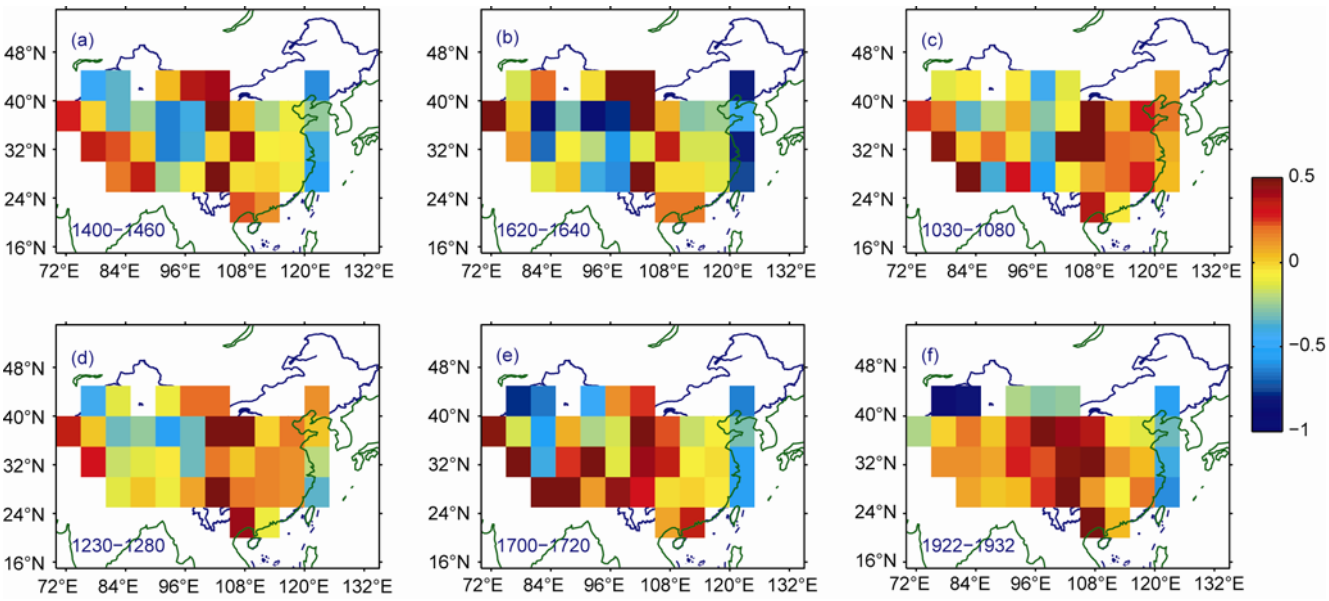


**Figure 5** Spatial patterns of temporally averaged temperature anomalies (with respect to 1961–1990) for selected periods. (a) 1400–1460, cold period; (b) 1620–1640, cold period; (c) 1030–1080 warm period; (d) 1230–1280, warm period; (e) 1700–1720, warm period; (f) 1922-1932, extreme drought.

a very similar pattern for eastern China over the last millennium. The pattern of the first three EOF modes of the observed data are however different. Therefore, the EOF analysis supports the idea that the spatial patterns of temperature variability in China changed over time.

The spatial variability of temperature anomalies-even between neighboring cells-highlights the risk of creating large errors in the climate reconstruction when using proxy data from a different grid cell. Accordingly, the correlation coefficients between the proxy data and the instrumental data are on average lower than for other palaeoclimatic field reconstructions [28], and many grid cells show low skill as measured by validation statistics (Table S2 in Appendix). The reason for these low skill values is the sparse distribution of proxy records. The sparse instrumental data in some regions may also be a part of the problem as the "target temperature" curve during the calibration period may sometimes not be adequate. Clearly, more proxy records and better instrumental data are needed to improve the skills of temperature reconstructions in China.

## 3 Conclusions

We have applied a point-by-point regression (PPR) framework combined with CPS and EIV approaches to generate the first spatially resolved temperature field reconstructions for China. Reconstructions were analyzed for spatial coherence of temperature anomalies on centennial and decadal time scales, and for variations in regional average temperature. The reconstruction using 415 paleo-temperature proxy records, shows that: 1) the late 20th century warming likely exceeds temperature levels at any period of the past 1000 years in China, 2) spatial heterogeneity is characteristic of the past temperature record in China, with between-cell correlation relatively highly variable in time, and 3) the climatic changes in the eastern and western regions of China over the past millennium are not synchronous during much of the last millennium. Our reconstructions may help provide a reference to test general circulation models simulating temperature variations over the past millennium.

The current limitations of our spatial temperature reconstruction are illustrated by the low reconstruction skill in some grid points, specifically, only 36 of 58 CPS grid points pass the RE validation. The major limiting factor is the low resolution and regional representation of the proxy data. Our results highlight the need for additional high-quality and long paleoclimate proxy records to reconstruct seasonally and annually resolved temperature fields in China. However, the limitations of the current reconstruction do not affect the main conclusion that the spatial mode of temperature has dramatically changed over time. Moreover, in the proxy data regression process, it is important to consider not only the significance of correlation between instrumental and proxy data, but also the geographical proximity of proxy data to grid points. A restricted search range, as we used it in this study, is likely to yield reconstructions less prone to distortion from nonstationarity of spatial temperature modes, and to yield reconstructions that more realistically reflect the temperature patterns of the past millennium.

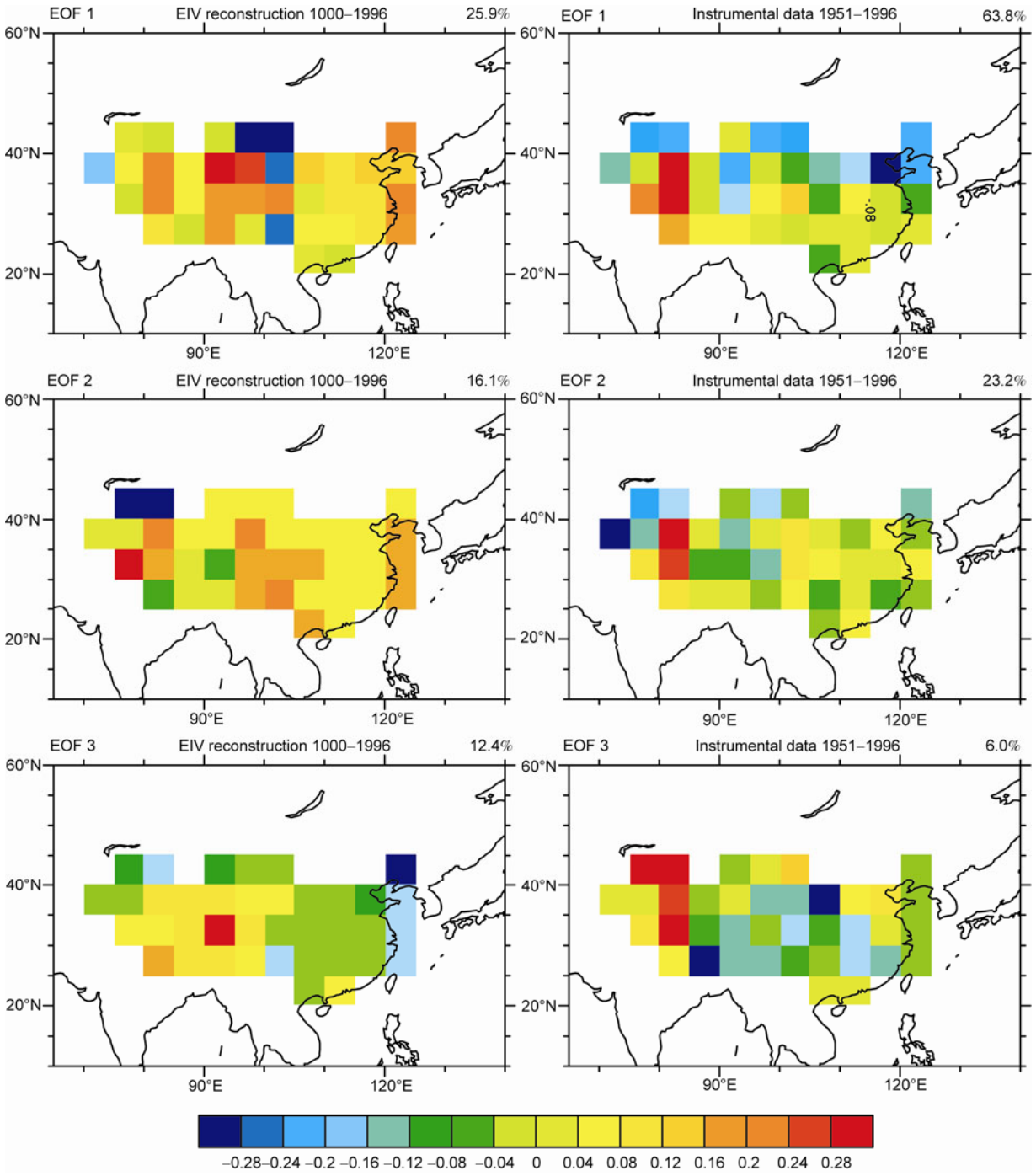


**Figure 6** Empirical orthogonal function (EOF) analysis of temperature anomalies (with respect to 1961–1990) for the EIV reconstruction in AD 1000–1996 and instrumental data in AD 1951–1996.

*We thank three anonymous reviewers for their thoughtful and constructive comments. We are also grateful to Quansheng Ge, Jingyun Zheng, Chun Qin, Zexin Fan, Keyan Fang, Achim Brauning, Jiangfeng Li, Yujiang Yuan, Xuemei Shao, Hongbing Liu, Yu Liu, Qibing Zhang, Paul Krusic, Jinbao Li, Jianfeng Peng, Xiaohua Gou, Haifeng Zhu, Edward Cook, Shaowu Wang, Deer Zhang, Ming Tan, Paul Sheppard and other scientists who have contributed their proxy data in the study region to the publicly available database. The study was supported by the CAS Strategic Priority Research Program (Grant No. XDA05080801), the National Basic Research Program of China (Grant No. 2010CB950104), the Chinese Academy of Sciences 100 Talents Project (Grant No. 29082762), and the National Natural Science Foundation of China (Grant No. 40871091). Feng Shi was supported by the West Light Program for Talent Cultivation of Chinese Academy of Sciences and China Meteorological Administration Drought Research Fund (Grant Nos. IAM201213 and IAM201109). Lucien von Gunten was supported by the Swiss NSF (Grant No. PBBEP2-126056). We also thank Dr. David M. Meko for reading an initial draft of the manuscript and providing numerous suggestions for improvement.*

1 Crowley T J. Causes of climate change over the past 1000 years. Science, 2000, 289: 270–277

2 Crowley T J, Lowery T S. How warm was the medieval warm period? Ambio, 2000, 29: 51–54
3 Briffa K R, Osborn T J, Schweingruber F H, et al. Low-frequency temperature variations from a northern tree ring density network. J Geophys Res, 2001, 106: 2929–2941
4 Esper J, Cook E, Schweingruber F. Low-frequency signals in long tree-ring chronologies for reconstructing past temperature variability. Science, 2002, 295: 2250–2253
5 Moberg A, Sonechkin D M, Holmgren K, et al. Highly variable Northern Hemisphere temperatures reconstructed from low- and high-resolution proxy data. Nature, 2005, 433: 613–617
6 Mann M E, Zhang Z H, Rutherford S, et al. Global signatures and dynamical origins of the Little Ice Age and Medieval climate anomaly. Science, 2009, 326: 1256–1260
7 Ljungqvist F C, Krusic P J, Brattström G, et al. Northern Hemisphere temperature patterns in the last 12 centuries. Clim Past 2012, 8: 227–249
8 Casty C, Raible C C, Stocker T F, et al. A European pattern climatology 1766–2000. Clim Dynam, 2007, 29: 791–805
9 Guiot J, Nicault A, Rathgeber C, et al. Last-millennium summer-temperature variations in western Europe based on proxy data. Holocene, 2005, 15: 489–500
10 Luterbacher J, Dietrich D, Xoplaki E, et al. European seasonal and annual temperature variability, trends, and extremes since 1500. Science, 2004, 303: 1499–1503
11 Pauling A, Luterbacher J, Casty C, et al. Five hundred years of gridded high-resolution precipitation reconstructions over Europe and the connection to large-scale circulation. Clim Dynam, 2006, 26: 387–405
12 Riedwyl N, Kuttel M, Luterbacher J, et al. Comparison of climate field reconstruction techniques: Application to Europe. Clim Dynam, 2009, 32: 381–395
13 Cook E, Woodhouse C, Eakin C, et al. Long-term aridity changes in the western United States. Science, 2004, 306: 1015–1018
14 Neukom R, Luterbacher J, Villalba R, et al. Multi-centennial summer and winter precipitation variability in southern South America. Geophys Res Lett, 2010, 37, doi: 10.1029/2010GL043680
15 Neukom R, Luterbacher J, Villalba R, et al. Multiproxy summer and winter surface air temperature field reconstructions for southern South America covering the past centuries. Clim Dynam, 2011, 37: 35–51
16 Wang S W, Wen X Y, Luo Y, et al. Reconstruction of temperature series of China for the last 1000 years. Chin Sci Bull, 2007, 52: 3272–3280
17 Yang B, Braeuning A, Johnson K, et al. General characteristics of temperature variation in China during the last two millennia. Geophys Res Lett, 2002, 29: 38–31
18 Ge Q S, Zheng J Y, Hao Z X, et al. Temperature variation through 2000 years in China: An uncertainty analysis of reconstruction and regional difference. Geophys Res Lett, 2010, 37, doi: 10.1029/2009gl041281
19 Ge Q, Zheng J, Fang X, et al. Winter half-year temperature reconstruction for the middle and lower reaches of the Yellow River and Yangtze River, China, during the past 2000 years. Holocene, 2003, 13: 933–940
20 Liu Y, An Z, Linderholm H, et al. Annual temperatures during the last 2485 years in the mid-eastern Tibetan Plateau inferred from tree rings. Sci China Ser D-Earth Sci, 2009, 52: 348–359
21 Tan M, Liu T, Hou J, et al. Cyclic rapid warming on centennial-scale revealed by a 2650-year stalagmite record of warm season temperature. Geophys Res Lett, 2003, 30: 1617–1620
22 Yao T D, Guo X J, Thompson L, et al. $\delta^{18}$O record and temperature change over the past 100 years in ice cores on the Tibetan Plateau. Sci China Ser D-Earth Sci, 2006, 49: 1–9
23 Shao X, Wang S, Zhu H, et al. A 3585-year ring-width dating chronology of Qilian juniper from the northeastern Qinghai-Tibetan Plateau. Iawa J, 2009, 30: 379–394
24 Zhang Y, Gou X, Chen F, et al. A 1232-year tree-ring record of climate variability in the Qilian Mountains, northwestern China. Iawa J, 2009, 30: 407–420
25 Liu X, Shao X, Zhao L, et al. Dendroclimatic temperature record derived from tree-ring width and stable carbon isotope chronologies in the Middle Qilian Mountains, China. Arct Antarct Alp Res, 2007, 39: 651–657
26 Zhang Q B, Cheng G D, Yao T D, et al. A 2,326-year tree-ring record of climate variability on the northeastern Qinghai-Tibetan Plateau. Geophys Res Lett, 2003, 30: 1739–1742
27 Bradley R S. Paleoclimatology: Reconstructing Climates of the Quaternary. 2rd ed. London: Academic Press, 1999
28 Cook E R, Meko D M, Stahle D W, et al. Drought reconstructions for the continental United States. J Clim, 1999, 12: 1145–1162
29 Cook E R, Anchukaitis K J, Buckley B M, et al. Asian monsoon failure and megadrought during the last millennium. Science, 2010, 328: 486–489
30 Zheng J, Yin Y, Li B. A new scheme for climate regionalization in China (in Chinese). Acta Geogr Sin, 2010, 65: 3–12
31 Brohan P, Kennedy J, Harris I, et al. Uncertainty estimates in regional and global observed temperature changes: A new dataset from 1850. J Geophys Res, 2006, 111, doi: 10.1029/2005JD006548
32 Li Q X, Dong W J, Li W, et al. Assessment of the uncertainties in temperature change in China during the last century. Chin Sci Bull, 2010, 55: 1974–1982
33 Fang K Y, Gou X H, Chen F H, et al. Large-Scale Precipitation Variability over Northwest China Inferred from Tree Rings. J Clim, 2011, 24: 3457–3468
34 Zhu H, Zheng Y, Shao X, et al. Millennial temperature reconstruction based on tree-ring widths of Qilian juniper from Wulan, Qinghai Province, China. Chin Sci Bull, 2008, 53: 3914–3920
35 Liu Y, An Z, Ma H, et al. Precipitation variation in the northeastern Tibetan Plateau recorded by the tree rings since 850 AD and its relevance to the Northern Hemisphere temperature. Sci China Ser D-Earth Sci, 2006, 49: 408–420
36 Briffa K R, Melvin T M. A closer look at regional curve standardization of tree-ring records: Justification of the need, a warning of some pitfalls, and suggested improvements in its application. In: Hughes M K, Swetnam T W, Diaz H F, eds. Dendroclimatology: Progress and Prospects. Heidelberg: Springer, 2011. 113–145
37 Yang B. Spatial and temporal patterns of climate variations over the Tibetan Plateau during the period 1300–2010 (in Chinese). Quat Sci, 2012, 32: 81–94
38 Yi L, Yu H, Ge J, et al. Reconstructions of annual summer precipitation and temperature in north-central China since 1470 AD based on drought/flood index and tree-ring records. Clim Change, 2011, 110: 469–498
39 Li Z S, Zhang Q B, Ma K. Tree-ring reconstruction of summer temperature for AD 1475–2003 in the central Hengduan Mountains, Northwestern Yunnan, China. Clim Change, 2011, 110: 455–467
40 Christiansen B, Ljungqvist F C. Reconstruction of the extratropical NH mean temperature over the last millennium with a method that preserves low-frequency variability. J Clim, 2011, 24: 6013– 6034
41 Yang B, Qin C, Huang K, et al. Spatial and temporal patterns of variations in tree growth over the northeastern Tibetan Plateau during the period AD 1450–2001. Holocene, 2010, 20: 1235–1245
42 Yang B, Kang X C, Liu J J, et al. Annual temperature history in Southwest Tibet during the last 400 years recorded by tree rings. Int J Climatol, 2010, 30: 962–971
43 Yang B, Kang X C, Brauning A, et al. A 622-year regional temperature history of southeast Tibet derived from tree rings. Holocene, 2010, 20: 181–190
44 Fan Z, Brauning A, Tian Q, et al. Tree ring recorded May–August temperature variations since AD 1585 in the Gaoligong Mountains, southeastern Tibetan Plateau. Palaeogeogr Palaeoclimatol Palaeoecol, 2010, 296: 94–102
45 Tan L, Cai Y, Cheng H, et al. Summer monsoon precipitation variations in central China over the past 750 years derived from a high-resolution absolute-dated stalagmite. Palaeogeogr Palaeoclimatol Palaeoecol, 2009, 280: 432–439

46 Liang E, Shao X, Xu Y. Tree-ring evidence of recent abnormal warming on the southeast Tibetan Plateau. Theor Appl Climatol, 2009, 98: 9–18
47 Fan Z X, Brauning A, Yang B, et al. Tree ring density-based summer temperature reconstruction for the central Hengduan Mountains in southern China. Global Planet Change, 2009, 65: 1–11
48 Zhang P, Cheng H, Edwards R, et al. A test of climate, Sun, and culture relationships from an 1810-year Chinese cave record. Science, 2008, 322: 940–942
49 Mann M E, Zhang Z H, Hughes M K, et al. Proxy-based reconstructions of hemispheric and global surface temperature variations over the past two millennia. Proc Natl Acad Sci USA, 2008, 105: 13252–13257
50 Liang E, Shao X, Qin N. Tree-ring based summer temperature reconstruction for the source region of the Yangtze River on the Tibetan Plateau. Global Planet Change, 2008, 61: 313–320
51 Hu C, Henderson G M, Huang J, et al. Quantification of Holocene Asian monsoon rainfall from spatially separated cave records. Earth Planet Sc Lett, 2008, 266: 221–232
52 Fan Z, Brauning A, Cao K. Annual temperature reconstruction in the Central Hengduan Mountains, China, as deduced from tree rings (in Chinese). Dendrochronologia, 2008, 26: 97–107
53 Gou X H, Chen F H, Jacoby G, et al. Rapid tree growth with respect to the last 400 years in response to climate warming, northeastern Tibetan Plateau. Int J Climatol, 2007, 27: 1497–1503
54 Thompson L G, Yao T, Davis M E, et al. Holocene climate variability archived in the Puruogangri ice cap on the central Tibetan Plateau. Ann Glaciol, 2006, 43: 61–69
55 Thompson L G, Mosley-Thompson E, Brecher H, et al. Abrupt tropical climate change: Past and present. Proc Natl Acad Sci USA, 2006, 103: 10536–10543
56 Thompson L, Mosley-Thompson E, Davis M, et al. Tropical glacier and ice core evidence of climate change on annual to millennial time scales. Clim Change, 2003, 59: 137–155
57 Cook E R, Krusic P J, Jones P D. Dendroclimatic signals in long tree-ring chronologies from the Himalayas of Nepal. Int J Climatol, 2003, 23: 707–732
58 Esper J, Schweingruber F, Winiger M. 1300 years of climatic history for Western Central Asia inferred from tree-rings. Holocene, 2002, 12: 267–277
59 D'Arrigo R, Jacoby G, Frank D, et al. 1738 years of Mongolian temperature variability inferred from a tree-ring width chronology of Siberian pine. Geophys Res Lett, 2001, 28: 543–546
60 Thompson L, Yao T, Mosley-Thompson E, et al. A high-resolution millennial record of the South Asian monsoon from Himalayan ice cores. Science, 2000, 289: 1916
61 Li J, Yuan Y, You X. The Tree-ring Hydrology Research and Application (in Chinese). Beijing: Science Press, 2000
62 Liu H B, Shao X M. Reconstruction of earlyspring temperature at Zhenan from 1755 using tree ring chronology (in Chinese). Acta Meteorol Sin, 2000, 58: 223–234
63 Shao X, Fan J. Past climate on west Sichuan Plateau as reconstructed from ring-widths of dragon spruce (in Chinese). Quat Sci, 1999, 1: 81–89
64 Ku T L, Li H C. Speleothems as high-resolution paleoenvironment archives: Records from northeastern China. P Indian Earth, 1998, 107: 321–330
65 Kitagawa H, Matsumoto E. Climatic implications of $\delta^{13}$C variations in a Japanese cedar (*Cryptomeria japonica*) during the last two millenia. Geophys Res Lett, 1995, 22: 2155–2158
66 Wang W C, Portman D, Gong G, et al. Beijing summer temperatures since 1724. In: Bradley R S, Jones P D, eds. Climate since A. D. 1500. London and New York: Routledge, 1992. 679
67 Wang R, Wang S, Fraedrich K. An approach to reconstruction of temperature on a seasonal basis using historical documents from China. Int J Climatol, 1991, 11: 381–392
68 Wang S, Wang R. Seasonal and annual temperature variations since 1470 AD in East China (in Chinese). Acta Meteorol Sin, 1990, 4: 428–439
69 Zhang D. Winter temperature changes during the last 500 years in South China. Chin Sci Bull, 1980, 25: 497–500
70 Zhang Q, Gemmer M, Chen J. Climate changes and flood/drought risk in the Yangtze Delta, China, during the past millennium. Quatern Int, 2008, 176–177: 62–69
71 Bräuning A, Grießinger J. Late Holocene variations in monsoon intensity in the Tibetan-Himalayan region—Evidence from tree rings. J Geol Soc India, 2006, 68: 485–493
72 Wang Y, Cheng H, Edwards R L, et al. The Holocene Asian Monsoon: Links to solar changes and north atlantic climate. Science, 2005, 308: 854–857
73 Qian W, Hu Q, Zhu Y, et al. Centennial-scale dry-wet variations in East Asia. Clim Dynam, 2003, 21: 77–89
74 Zhang P, Gong G. Some characteristics of climatic fluctuations in China since the 16th century. Acta Meteorol Sin, 1979, 34: 238–247
75 Cook E R, Seager R, Cane M A, et al. North American drought: Reconstructions, causes, and consequences. Earth-Sci Rev, 2007, 81: 93–134
76 Schneider T. Analysis of incomplete climate data: Estimation of mean values and covariance matrices and imputation of missing values. J Clim, 2001, 14: 853–871
77 Jones P D, Briffa K R, Osborn T J, et al. High-resolution palaeoclimatology of the last millennium: A review of current status and future prospects. Holocene, 2009, 19: 3–49
78 Mann M E, Rutherford S, Wahl E, et al. Robustness of proxy-based climate field reconstruction methods. J Geophys Res, 2007, 112, doi: 10.1029/2006jd008272
79 Riedwyl N, Luterbacher J, Wanner H. An ensemble of European summer and winter temperature reconstructions back to 1500. Geophys Res Lett, 2008, 35, doi: 10.1029/2008gl035395
80 Rutherford S, Mann M E, Osborn T J, et al. Proxy-based Northern Hemisphere surface temperature reconstructions: Sensitivity to method, predictor network, target season, and target domain. J Clim, 2005, 18: 2308–2329
81 McShane B B, Wyner A J. A statistical analysis of multiple temperature proxies: Are reconstructions of surface temperatures over the last 1000 years reliable? Ann Appl Stat, 2011, 5: 5–44
82 Lee T C K, Zwiers F W, Tsao M. Evaluation of proxy-based millennial reconstruction methods. Clim Dynam, 2008, 31: 263–281
83 Jones P D, Briffa K R, Barnett T P, et al. High-resolution palaeoclimatic records for the last millennium: Interpretation, integration and comparison with General Circulation Model control-run temperatures. Holocene, 1998, 8: 455–471